

**THE LUNAR FORMATION INA: A SCENARIO OF ORIGIN.** Yu. Shkuratov<sup>1</sup>, V. Kaydash<sup>1</sup>, S. Velichko<sup>1</sup>, V. Korokhin<sup>1</sup>, E. Surkov<sup>1</sup>, Yu. Velikodsky<sup>2</sup>, G. Videen<sup>3</sup>, <sup>1</sup>Institute of Astronomy of V.N. Karazin Kharkiv National University, Sumska 35, 61022 Kharkiv, Ukraine, <sup>2</sup>National Aviation University, Lubomyr Husar Ave. 1, Kyiv 03058, Ukraine, <sup>3</sup>Space Science Institute, Boulder, Colorado, USA.

**Introduction:** Ina is located on the top of a shield volcano that has a size of about 20 km and height near 300 m [1] (Fig. 1). Estimates of the crater distribution density show that the age of the volcanic edifice is about 3.5 Ga [1,2,3,6]. Ina is a collapsing structure. The *D*-shaped depression has a size of approximately 2×3 km and a depth near the center of about 60 m (Fig. 2). Flat-topped but steeply edged hills of a height of 5-20 m are seen inside this formation. This is comparable with the thickness of the regolith layer of old lunar surfaces. The shape of the hills is irregular, although rounded. The hills are separated by freshly looking hummocky relief (HR) with a height drop of a few meters. Moat-like structures are seen between the HR areas and hills (Fig. 2). The craters density reveals that the Ina hills are young, <100 Ma [1-8].

A few scenarios of Ina's surface origin exist [1-8]. A popular one is that the Ina hills are inflation mounds resulting from solidification of the extruded magmatic foam, which is due to the lava saturation with volatiles erupting into vacuum [1,5]. During cooling and degassing the eruptive foam forms mounds of high porosity (>75%) [1,5]. Penetrating meteorites produce craters of smaller diameters compared to the usual regolith layer. This may lead to underestimates of the absolute age of the hills.

**New hypothesis:** We suggest a model, in which the hills are not of extrusive origin, but are fragments of the old surface that survived lowering of several tens of meters in slow collapses that were triggered, e.g., by tectonic and moonquake effects or heating lava that may episodically approach the volcano top. The vent and throat of the volcano can have voids after former eruptions, providing the possibility of a roof collapse. Portions of the old surface could be destroyed in their fall, while other surface fragments survived. During the collapses, a large quantity of craters on the hill surface would disappear due to catastrophic vertical and horizontal moves of the blanketing regolith. Such movements can produce the rounded upper edges of the hills (Fig. 2). When the event occurred, e.g., near 33 Ma [8], new craters formed on the hill surface, but with a smaller spatial density. The material of the portion of destroyed roof mixed with the lava material during the extrusive activity, forming the HR surface that is almost without craters and regolith. The composition difference of the HR areas may be caused by chemical differentiation in the lava source during an extended period [2]. In the considered scenario the term "inflation mounds" [4],

i.e. the deformation of hardened top layer under the pressure of liquid lava from below, is more suitable to the HR, than to hills formed by the surviving surface that partially preserved the regolith.

**Arguments to the scenario:** To study Ina, we used *LRO NAC* data to characterize structure features [9,10] and *MI Kaguya* images to assess chemical composition and maturity degree by the Lucey method. In the latter case, to use the Lucey et al. formulas [11,12], we connected the *MI Kaguya* photometric system to the *Clementine* one.

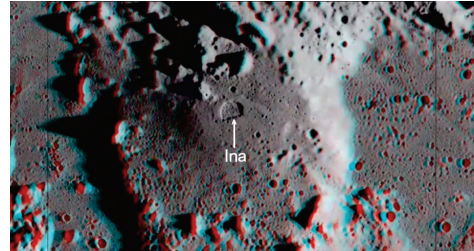


Figure 1. An anaglyph of the shield volcano with the crater Ina on the top indicated with the arrow (18.65°N, 5.30°E).

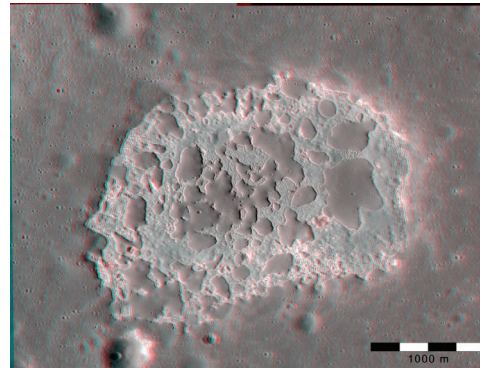


Figure 2. An anaglyph of the Ina formation.

Figures 3a-c show images of the equigonal albedo  $A_{eq}(\alpha)$  [9] at different phase angles. Notable differences between the Ina patterns exist. At small phase angles, where the influence of structure is minimal, the HR surface is darker than the hills. This suggests the albedo difference is due to chemical composition. At larger phases, one may observe even inversion of albedo contrast. Figure 3d shows the phase ratio  $A_{eq}(91.1^\circ)/A_{eq}(5.7^\circ)$  ruled by the surface microstructure. The ratio shows resemblance of the microstructure of the hills and terrain around Ina. The HR areas notably differ from the hills, demonstrating high homogeneity. Note that other phase ratios, e.g.,  $A_{eq}(90.1^\circ)/A_{eq}(34.7^\circ)$  or  $A_{eq}(34.7^\circ)/A_{eq}(5.7^\circ)$ , are similar.

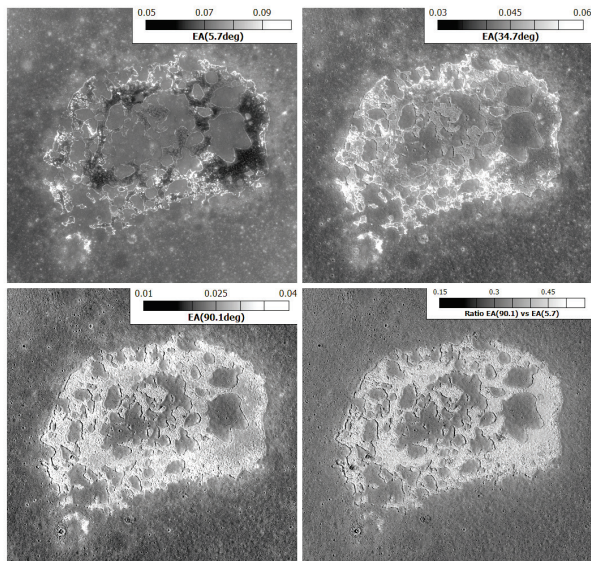


Figure 3. Images of the equigonal albedo (EA) for the formation Ina obtained at  $\alpha = 5.7^\circ$ ,  $34.7^\circ$ , and  $90.1^\circ$ , respectively, (a) – (c). The phase ratio  $A_{\text{eq}}(90.1^\circ)/A_{\text{eq}}(5.7^\circ)$  is shown in (d).

We calculated phase curves for four sites of the Ina area (Fig. 4). The points 1 and 2 represent the hills and HR, respectively. The phase curve of Point 1 has significantly smaller slope, as would been anticipated from Fig. 3d. It is interesting that both points are located at the equal heights (Fig. 5a). Points 2 and 3 have very similar phase curves, i.e. the crater densities of the hill surface and surrounding Ina surface are different, but the microstructure of their regoliths is the same. For comparison, Point 4 shows the phase curve for a bright young crater. If we suggest that the age of the hills is near 30 Ma [8], then, the phase-curve similarity of Point 1 and 2 suggests that the fairy-castle microstructure [13] producing the regolith backscatter is formed rather quickly in time  $<30$  Ma. Thus, the small slope of phase curves of the HR areas is indeed ruled by the microstructure; their complicated relief does not perceptibly affect the backscattering. We may suppose that the surface of the areas is almost regolith-free and have an age of a few million years.

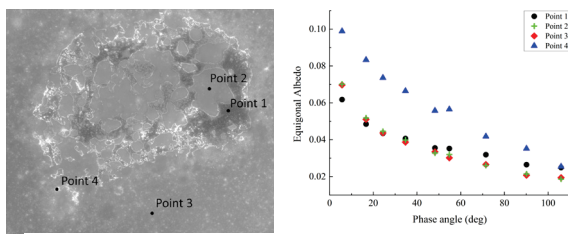


Figure 4. The locations of the points (left), for which the phase curves were calculated (right).

Figure 5 displays results of our calculations of the FeO and TiO<sub>2</sub> contents and the parameter OMAT, using the Lucey et al. technique [11,12]. The OMAT

reveals inverse correlations with maturity degree. In Fig. 5b one may see that the surfaces of hills and surrounding Ina areas have almost the same high maturity, whereas, the HR areas have conspicuously lower maturity degree. The areas are also characterized with high content of TiO<sub>2</sub> and a bit larger abundance of FeO. Moreover, Ina is surrounded by a bluish halo [2] that, perhaps, is a deposit material pulverized at the latest eruption. This deposit contains TiO<sub>2</sub> in high quantity. Several craters in Ina's vicinity also have bluish halos. This can indicate that near the surface of the volcano there may be hidden volcanic tubes and sills, containing high-titanium lava, that were unsealed by the impacts at the craters' formation.

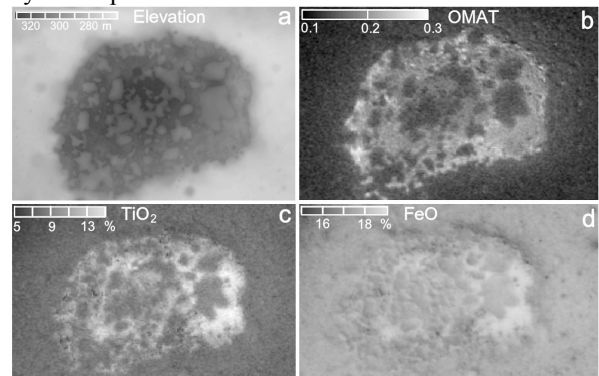


Figure 5. The formation Ina: (a) digital elevation data of the LRO LOLA altimeter, (b) – (d) correspond to, respectively, the parameter OMAT, TiO<sub>2</sub> and FeO contents assessed by the Lucey technique [11,12].

**Conclusion:** We propose a scenario of crater Ina formation, according to which the hills on the crater floor are portions of the old surface that survived a collapse. In this catastrophe the hill surface would lose craters and an amount of the regolith. The HR terrains are formed due to debris of the fallen roof and extrusion lava that may uplift much later than the roof collapse. During the extrusion in the zones of the contacts of the extrusion mass and hills, moat-like structures may appear. They are observed in Fig. 5a.

**References:** [1] Qiao Le. et al. (2017) *Geology* 45, 455–458. [2] Strain P. & El Baz F. (1980) *Proc. LPSC XI*, 2437–2446. [3] Schultz P. et al. (2006) *Nature* 444, 184–186. [4] Garry W. et al. (2012) *JGR* 117, E00H31. [5] Wilson L. & Head J. (2017) *Volcan. Geotherm. Res.* 335, 113–127. [6] Braden S. et al. (2014) *Nature Geosci.* 7, 787–791. [7] Basilevsky A.T. & Michael G.G. (2021), *Sol. Sys. Res* 55, 20. [8] Qiao Le. et al. (2021) *Planet. Sci. Journ.* 2:66 13pp. [9] Shkuratov Yu. et al. (2011) *PSS* 59, 1326–1371. [10] Kaydash V. et al. (2012) *JQSRT* 113, 2601–2607. [11] Lucey P. et al. (1995) *Science* 268, 1150–1153. [12] Blewett D. et al. (1997) *JGR* 102, 16319–16325. [13] Hapke B. (2012) *Theory of Reflectance and Emittance Spectroscopy*. Cambridge Univ. Press.